Equilibrium and Dynamic Bilayer Structural Properties of Unsaturated Acyl Chain Phosphatidylcholine–Cholesterol–Rhodopsin Recombinant Vesicles and Rod Outer Segment Disk Membranes As Determined from Higher Order Analysis of Fluorescence Anisotropy Decay†

Martin Straume‡ and Burton J. Litman*

Department of Biochemistry, University of Virginia School of Medicine, Charlottesville, Virginia 22908

Received January 29, 1988; Revised Manuscript Received June 14, 1988

ABSTRACT: Limited-frequency phase-modulation fluorometry of diphenylhexatriene (DPH) and trimethylammonium–diphenylhexatriene (TMA–DPH) was used to characterize the equilibrium and dynamic lipid structural properties of (1) reconstituted egg phosphatidylcholine (egg PC)–rhodopsin vesicles varying in rhodopsin content from 0 to ~1 mol %, (2) reconstituted PC–cholesterol–rhodopsin vesicles containing ~1 mol % rhodopsin and 0, ~15, or ~30 mol % cholesterol with egg PC, DOPC (di-18:1-PC), or PAPC (16:0,20:4-PC) as the phospholipid constituent, and (3) native bovine rod outer segment disk membranes. Experiments were conducted at 37, 25, 15, and 5 °C. Fluorescence lifetime analysis was performed by fitting the data to a constrained, discrete, biexponential model. Rotational depolarization properties were considered by a model requiring a single rotational diffusion coefficient and capable of producing orthogonal, bimodal orientational distributions for DPH and unimodal distributions for TMA–DPH [Straume, M., & Litman, B. J. (1987) *Biochemistry 26*, 5113–5120]. Unbleached rhodopsin reduced mean fluorophore lifetimes in proportion to the amount of protein present in PC vesicles as a result of probe-to-retinal energy transfer by (1) redistributing the relative lifetime contributions in favor of the short lifetime population and (2) reducing the lifetimes of each derived population. Lifetimes were increased by cholesterol and by reduction of the temperature, but the relative proportions of derived short- and long-lifetime populations were not affected. TMA–DPH lifetimes were more sensitive (in a relative manner) than were those of DPH. These observations are interpreted in terms of cholesterol and reduced temperature each inhibiting water penetrability into these bilayers, with a greater effect occurring in the headgroup and interfacial regions (probed by TMA–DPH) than in the hydrophobic bilayer interior (probed by DPH). Diunsaturated DOPC–rhodopsin recombinants were more resistant to temperature-dependent lifetime changes than were mixed-chain egg PC or PAPC vesicles. This suggests less favorable interaction of rhodopsin with diunsaturated PCs than with mixed-chain PCs. Lifetimes in disk membranes exhibited this same temperature dependence although DPH in disks had lifetimes longer than those seen in recombinant vesicles. TMA–DPH lifetimes in disks were more similar to those observed in cholesterol-containing recombinants. It would therefore appear that the large proportion of small, charged (at pH 7) phosphatidylethanolamine and phosphatidylserine headgroups present in disks reduces water penetrability into the disk membrane, with a greater effect observed in the hydrophobic bilayer interior. Equilibrium lipid ordering was increased in proportion to (1) vesicle rhodopsin content, (2) vesicle cholesterol content, and (3) extent of temperature reduction. Unimodal TMA–DPH orientational distributions were narrowed whereas the bimodal distributions of DPH were primarily redistributed in favor of alignment with the phospholipid acyl chains while not being as substantially narrowed. Rhodopsin, cholesterol, and reduced temperature, therefore, each increased the lateral lipid packing density and induced a more extended average configuration of the acyl chain termini in these membranes. Diunsaturated DOPC–rhodopsin recombinants containing no cholesterol showed less rhodopsin-dependent lipid ordering of the headgroup and interfacial regions than did equivalent mixed-chain egg PC or PAPC vesicles. This is again consistent with less favorable interaction of rhodopsin with unsaturated acyl chain PCs than with those containing saturated acyl chains. Cholesterol eliminated this acyl chain dependent difference. Equilibrium lipid order in disk membranes was most similar to that seen in cholesterol-containing recombinant vesicles. Fluorophore rotational dynamics were independent of vesicle rhodopsin content, acyl chain composition, and depth within the bilayer. Cholesterol had little effect on probe depolarization dynamics in these rhodopsin-containing vesicles, in contrast to the considerable cholesterol-dependent acceleration observed in similar rhodopsin-free vesicles [Straume, M., & Litman, B. J. (1987) *Biochemistry 26*, 5121–5126]. Slower motions were consistently induced by temperature reductions.

Integral membrane proteins are involved in many functional roles critical to the activity of biological systems (Benga & Holmes, 1984; Salesse & Garnier, 1984; Thompson & Huang, 1986). Regulation of the functional properties of such proteins (or protein systems) can be influenced by various molecular interactions which can occur in biomembranes. The lipid matrices of natural membrane systems are composed of many molecular species which vary in their relative proportions depending on the tissues from which they are derived (Akino

† Supported by National Science Foundation Grant PCM-8316858 and National Institutes of Health Grant EY00548.

‡ Present address: Department of Pharmacology, University of Virginia School of Medicine, Charlottesville, VA 22908.

0006-2960/88/0427-7723$01.50/0

& Tsuda, 1979; Benga & Holmes, 1984; Miljanich et al., 1979; Thompson & Huang, 1986). The large proportion of unsaturated phospholipid acyl side chains in native bovine rod outer segment (ROS)[1] disk membranes (Anderson & Maude, 1970; Anderson & Sperling, 1971; Borggreven et al., 1970; Miljanich et al., 1979; Nielsen et al., 1970; Poincelot & Abrahamson, 1970), as well as that of most biological membrane systems (Akino & Tsuda, 1979; Benga & Holmes, 1984; Miljanich et al., 1979; Thompson & Huang, 1986), suggests that these natural membranes exist in the liquid-crystalline state at physiological temperatures. Cholesterol, also, is a common constituent of biological membranes and is found in varying proportions in different membranes. Compositional heterogeneity of the lipid fraction of biological membranes thus offers a means for regulating the physical properties of the bilayer, which, in turn, have an influence in mediating functional responses of membrane proteins (Applebury et al., 1974; Baldwin & Hubbell, 1985a,b; Deese et al., 1981; Devaux & Seigneuret, 1985; Jahnig et al., 1982; Litman et al., 1981; Morton et al., 1986; O'Brien et al., 1977; Salesse & Garnier, 1984; Stubbs & Litman, 1978; Stubbs et al., 1976). Since integral membrane proteins are responsible for most transmembrane phenomena in biological systems (Benga & Holmes, 1984; Salesse & Garnier, 1984; Thompson & Huang, 1986), it is of interest to characterize, in a controlled manner, the influence of a model, intrinsic membrane protein on the physical properties of reconstituted, liquid-crystalline lipid bilayers varying in acyl chain composition and cholesterol content. An understanding of the relationships between bilayer lipid composition and structural properties together with their associated influences on membrane protein functional behavior may then be developed to yield information about regulatory mechanisms at work in biomembranes.

Synthetic model lipid vesicles have been studied extensively as a means of characterizing the properties of compositionally less complex bilayers than those derived from natural sources. Differences in equilibrium and dynamic bilayer structure may thus systematically be determined as a function of phospholipid acyl chain and/or headgroup composition, cholesterol content, protein content, and temperature, for example. Much early work in this area focused on characterization of the gel to liquid-crystalline phase transition of saturated acyl chain phosphatidylcholine systems (Estep et al., 1978; Lakowicz, 1981, 1980; Lakowicz & Prendergast, 1978; Lakowicz et al., 1979; Shinitzky & Barenholz, 1978). More recently, greater emphasis has been placed on understanding the structural properties of unsaturated acyl chain bilayers (Stubbs et al., 1981). Characterization of subtle structural differences induced in synthetic liquid-crystalline vesicles by varying compositional parameters may permit correlation of detailed bilayer structural properties with molecular composition.

Molecular dynamics in bilayers have been observed to occur in the nanosecond time scale (Benga & Holmes, 1984; Brown & Williams, 1985; Devaux & Seigneuret, 1985; Stubbs, 1983; Thompson & Huang, 1986; Wong, 1984; Yeagle, 1984). Characterization of bilayer structural properties may be accomplished on a nanosecond time scale by use of dynamic fluorescence techniques (Lakowicz, 1983, 1981, 1980). Observation of the total fluorescence intensity decay kinetics in addition to the dynamics of fluorescence anisotropy decay of the rod-like membrane probes DPH and TMA–DPH allows information to be extracted about the penetrability of water into bilayers (Straume & Litman, 1987a,b) and about the extents and rates of lipid structural fluctuations in two different regions of bilayer membranes (Ameloot et al., 1984; Barrow & Lentz, 1985; Engel & Prendergast, 1981; Jahnig et al., 1982; Kinosita et al., 1981a,b; Lakowicz et al., 1985; Parasassi et al., 1984; Pink et al., 1984; Prendergast et al., 1981; Straume & Litman, 1987a,b; Stubbs et al., 1984, 1981; van Blitterswijk et al., 1981; van de Ven et al., 1984; Vos et al., 1983). DPH, an entirely hydrophobic molecule, reports on the hydrophobic acyl side chain bilayer interior (Lakowicz, 1983; Shinitzky & Barenholz, 1978) whereas the amphipathic TMA–DPH molecule permits information to be obtained about the membrane headgroup and interfacial regions (Ameloot et al., 1984; Engel & Prendergast, 1981; Prendergast et al., 1981; Stubbs et al., 1984). The nearly collinear excitation and emission dipoles and long molecular axis of these probes make possible sensitive and relatively direct interpretation of fluorescence anisotropy decay phenomena (Lakowicz, 1983; Lipari & Szabo, 1980; Szabo, 1984; Zannoni et al., 1983). Fluorescence lifetimes of less than approximately 10 ns permit detection of nanosecond time scale dynamic quenching and rotational relaxation phenomena, allowing inference about the equilibrium and dynamic structure of the bilayer environment in the vicinity of these reporter molecules.

Fluorescence anisotropy decays have commonly been considered in terms of rotational correlation times and limiting anisotropies. These derived parameters do not have any direct physical significance in themselves, however. Physical interpretation has historically been limited to unimodal orientational distributions because of difficulty in deriving analytical expressions which account for anything beyond the second-rank order parameter. Interpretation of DPH rotational relaxation in the present work is accomplished by characterizing the orientational distribution of this probe by a higher order model than has commonly been used in the past. A bimodal orientational distribution function is invoked such that two orthogonal orientational populations of DPH may be derived (Ameloot et al., 1984; van der Meer et al., 1984). Such an interpretation is possible by considering not only the second-rank order parameter but also the fourth-rank order parameter. This interpretation is supported by variable-angle steady-state anisotropy experiments on oriented, planar bilayers (van de Ven et al., 1984; Vogel & Jahnig, 1985; Vos et al., 1983).

In the present studies, DPH is permitted to be distributed among two orthogonal orientational probability maxima of variable width, one aligned parallel to the bilayer normal and the other orthogonally oriented, lying parallel to the plane of the bilayer and located at the bilayer median (Straume & Litman, 1987a,b). TMA–DPH orientational properties are analyzed according to the same mathematical formalism except that all orientational probability is constrained within one probability maximum aligned parallel to the bilayer normal (Ameloot et al., 1984; Straume & Litman, 1987a,b). Application of such a higher order model to dynamic fluorescence depolarization measurements permits more detailed interpretation of the orientational redistribution of DPH in bilayer membranes, therefore potentially allowing a more detailed interpretation of lipid structural dynamics in the hydrophobic bilayer interior. Employing a common mathematical model for both probes allows a direct comparison of DPH and

[1] Abbreviations: $A_{280/500}$, ratio of 280-nm absorbance to that at 500 nm; DOPC, dioleoylphosphatidylcholine; DPH, diphenylhexatriene; DTPA, diethylenetriaminepentaacetate; egg PC, egg phosphatidylcholine; ESR, electron spin resonance; NMR, nuclear magnetic resonance; PAPC, palmitoylarachidonoylphosphatidylcholine; PC, phosphatidylcholine; PE, phosphatidylethanolamine; POPOP, 1,4-bis(5-phenyloxazol-2-yl)benzene; PS, phosphatidylserine; ROS, rod outer segment; TMA–DPH, trimethylammonium–diphenylhexatriene; ΔA_{500}, change in 500-nm absorbance.

TMA–DPH results. Of course, an assumption implicit in the use of extrinsically incorporated probes to monitor bilayers, such as DPH and TMA–DPH, is that they accurately report information about the equilibrium and dynamic structural properties of their local environment.

Recently reported studies employing the above-mentioned experimental and analytical methods have considered systematic changes in the equilibrium and dynamic bilayer structural properties of liquid-crystalline PC vesicles as related to acyl chain composition and cholesterol content as a function of temperature (Straume & Litman, 1987a,b). The present work (1) describes the effects of varying levels of the intrinsic membrane protein bovine rhodopsin on the structural properties of reconstituted egg PC–rhodopsin recombinant vesicles, (2) characterizes the properties of more compositionally complex ternary reconstituted PC–cholesterol–rhodopsin recombinants varying in acyl chain composition and cholesterol content, and (3) compares the properties of these reconstituted systems with results obtained from native bovine ROS disk membranes, all as a function of temperature. We thus (1) consider a variety of compositionally more complex, reconstituted, liquid-crystalline lipid–rhodopsin vesicle systems in which numerous compositional parameters are varied systematically and (2) analyze our experimental observations by applying a higher order model potentially capable of more detailed physical interpretation of bilayer structural dynamics than earlier, less sophisticated models.

Experimental Procedures

Disk Membrane and Rhodopsin Isolation. Isolation of native bovine rod outer segment (ROS) disk membranes and purification of unbleached rhodopsin by conconavalin A affinity chromatography of octyl glucoside solubilized disks was performed as described previously (Jackson & Litman, 1985; Litman, 1982; Smith et al., 1975) except that 50 μM DTPA (with 62.5 μM $MgCl_2$) was included in all buffers and solutions to minimize sample oxidation induced by any trace levels of iron.

Lipid–Rhodopsin Recombinant Vesicle Preparation. Large, unilamellar egg PC, DOPC, and PAPC lipid–rhodopsin recombinant vesicles containing 0, ~15, or ~30 mol % cholesterol and specified amounts of rhodopsin were prepared by an octyl glucoside dilution method (Jackson & Litman, 1985), with the modifications described in Straume and Litman (1987b) concerning the inclusion of cholesterol. Again, 50 μM DTPA and 62.5 μM $MgCl_2$ were included in all buffers and solutions.

Large, unilamellar egg PC vesicles containing no rhodopsin were prepared by octyl glucoside dialysis as described in Jackson et al. (1982) and Straume and Litman (1987a).

Total phospholipid concentrations were determined by phosphate analysis according to the method of Bartlett (1959).

Total protein concentrations were determined by the method of Lowry et al. (1951). Unbleached rhodopsin content was characterized by the change in 500-nm absorbance (ΔA_{500}) generated upon bleaching of samples by light. Preparations were solubilized in 1.5% cetyltrimethylammonium bromide (CTAB) in 0.1 M PO_4, pH 7, buffer, and 500-nm absorbances were determined before and after bleaching of the rhodopsin in the presence of hydroxylamine. Both the molar extinction coefficient at 500 nm and the molecular weight of rhodopsin are approximately 40 000 (Applebury, 1984; Applebury et al., 1974; Fukuda et al., 1979; Hargrave et al., 1983; Henselman & Cusanovich, 1974; Ovchinnikov, 1982). The observed ΔA_{500} was therefore approximately equivalent to the milligrams of unbleached rhodopsin per milliliter. The ratio of 280-nm absorbance to that at 500 nm ($A_{280/500}$) was also determined for unbleached aliquots to monitor the quality of rhodopsin samples. Low ratios (less than approximately 2.0) indicate relatively small amounts of unbleached rhodopsin and/or oxidized lipids. $A_{280/500}$ ratios typically observed for column-purified rhodopsin were approximately 1.7 and for recombinant vesicles were approximately 2.0.

Lipid peroxidation of PAPC samples was determined by 233-nm absorbance and thiobarbituric acid assay (Baker & Wilson, 1969; Slater, 1984; Sunamoto et al., 1985). No more than 0.5% peroxidation of PAPC samples was detected.

Cholesterol oxidase assays were employed to determine the cholesterol content of samples (Moore et al., 1977). Vesicle cholesterol content was always within a few mole percent of the desired 15 and 30 mol % levels.

Fluorescence Measurements. All vesicle samples were diluted to 0.5 mM phospholipid and labeled to 250:1 (mol/mol) DPH:phospholipid or 150:1 (mol/mol) TMA–DPH:phospholipid in rhodopsin-containing systems and 500:1 (mol/mol) DPH:phospholipid or 250:1 (mol/mol) TMA–DPH:phospholipid in rhodopsin-free systems as described in Straume and Litman (1987a). Samples were equilibrated at 37 °C in an SLM-4800 limited-frequency phase-modulation dynamic spectrofluorometer, and steady-state and dynamic measurements were performed at 37, 25, 15, and 5 °C [see Straume and Litman (1987a)].

Steady-state anisotropies were measured as were the phase angle shifts and relative amplitude demodulations characteristic of total fluorescence intensity decay kinetics and dynamic rotational depolarization properties exhibited by the probes. Excitation was by 360-nm light passed through 1-nm band-pass slits, and emission was at 430 nm after passage through 16-nm band-pass slits. Dual grating monochromators were employed for wavelength selection, and Glan-Thomson polarizers were used in the excitation and emission channels. Steady-state anisotropies were corrected for all instrumental factors. All dynamic measurements were made relative to a POPOP–absolute ethanol reference solution (Lakowicz, 1980). Unlabeled samples showed less than 1% background intensity under the conditions of the measurements. Rhodopsin-containing samples experienced no detectable bleaching of the protein as a result of the measurements.

Methods of Analysis. Total fluorescence intensity decay behavior was analyzed according to

$$I_{tot}(t) = \sum_{i=1}^{2} \alpha_i \exp\left(-\frac{t}{\tau_i}\right)$$

$$\alpha_2 = 1 - \alpha_1 \text{ (fractional amplitudes)}$$

$$\tau_2 = 4\tau_1 \text{ (fluorescence lifetimes)}$$

The constraint imposed on the τ_2/τ_1 ratio was derived from numerous reports in the literature based on lifetime behavior obtained from biexponential analysis of DPH in lipid bilayers (Ameloot et al., 1984; Chen et al., 1977; Hildenbrand & Nicolau, 1979; Kawato et al., 1977; Kinosita et al., 1981a,b; Klausner et al., 1980; Lakowicz et al., 1985; Parasassi et al., 1984; Stubbs et al., 1984, 1981). Use of parameters obtained at limited modulation frequencies made necessary imposition of this constraint to eliminate occasional convergence to physically unreasonable parameter values [see Straume and Litman (1987a)]. Results derived via this model agreed well with previously reported intensity decay behavior. The intensity-weighted mean fluorescence lifetime, $\tau(1)$, was used to characterize average intensity decay kinetics and is defined as

$$\tau(1) = \frac{1}{\langle\tau\rangle}\sum_{i=1}^{2}\alpha_i\tau_i^2 \qquad \langle\tau\rangle = \sum_{i=1}^{2}\alpha_i\tau_i$$

Rotational depolarization properties of the fluorophores were characterized by interpreting the parameters characteristic of the dynamics of anisotropy decay (i.e., steady-state anisotropy and differential phase angle shifts as a function of modulation frequency) within the framework of a mathematical model yielding bimodal equilibrium orientational distributions for DPH (Ameloot et al., 1984; Straume & Litman, 1987a,b; van der Meer et al., 1984; van de Ven et al., 1984; Vogel & Jahnig, 1984; Vos et al., 1983) and unimodal distributions for TMA–DPH (Ameloot et al., 1984; Straume & Litman, 1987a,b). The model employed characterizes the equilibrium and dynamic orientational properties of DPH and TMA–DPH by (1) the Gaussian distribution width of the orientational probability maxima θ_g, (2) the fraction of probe probability occupying the parallel orientational probability maximum $f_\parallel$ (i.e., that oriented parallel to the phospholipid acyl chains), and (3) the perpendicular rotational diffusion coefficient $D_\perp$ (Straume & Litman, 1987a,b). The equilibrium orientational distribution function employed for interpretation in the present work has the form

$$f(\theta) = \frac{\beta^2}{2}\left[\exp\left[-\left(\frac{\theta}{\theta_g}\right)^2\right] + \exp\left[-\left(\frac{\pi-\theta}{\theta_g}\right)^2\right]\right] + (1-\beta)^2\exp\left[-\left[\frac{(\pi/2)-\theta}{\theta_g}\right]^2\right]$$

$$f_\parallel = \frac{1}{N}\int_0^\pi f_\parallel(\theta)\sin\theta\,d\theta$$

$$f_\parallel(\theta) = \frac{\beta^2}{2}\left[\exp\left[-\left(\frac{\theta}{\theta_g}\right)^2\right] + \exp\left[-\left(\frac{\pi-\theta}{\theta_g}\right)^2\right]\right]$$

$$N = \int_0^\pi f(\theta)\sin\theta\,d\theta$$

The value of β was constrained to 1.0 in the case of TMA–DPH-labeled samples, thus producing a value of 1.0 for $f_\parallel$ and modeling no orthogonal distribution of TMA–DPH in the bilayers (Ameloot et al., 1984; Straume & Litman, 1987a,b). The two parameters β and θ_g defined $f(\theta)$ to permit analysis of anisotropy decay parameters according to the model derived by van der Meer et al. (1984) which predicts

$$r(t) = b_4 + \sum_{j=1}^{3} b_j \exp\left(-\frac{t}{\phi_j}\right)$$

where $r(t)$ = time dependence of fluorescence anisotropy decay; b_1, b_2, b_3 = functions of $\langle P_2\rangle$ and $\langle P_4\rangle$; b_4 = function of $\langle P_2\rangle$; ϕ_1, ϕ_2, ϕ_3 = functions of $\langle P_2\rangle$, $\langle P_4\rangle$, and $D_\perp$; $\langle P_2\rangle$ = second-rank Legendre order parameter; $\langle P_4\rangle$ = fourth-rank Legendre order parameter; $D_\perp$ = perpendicular rotational diffusion coefficient; $\langle P_k\rangle = (1/N)\int_0^\pi f(\theta)P_k(\cos\theta)\,d\theta$ (k = 2, 4); $P_2(\cos\theta) = (3\cos^2\theta - 1)/2$; and $P_4(\cos\theta) = (35\cos^4\theta - 30\cos^2\theta + 3)/8$.

Overall equilibrium ordering experienced by the probes was quantified by the fractional volume parameter f_v, which characterizes the volume available for probe reorientational motion relative to that available in an unhindered, isotropic probe environment (Straume & Litman, 1987a,b). This parameter is defined as

$$f_v = \frac{1}{2f(\theta)_{max}}\int_0^\pi f(\theta)\sin\theta\,d\theta$$

Simultaneous interpretation of θ_g and $f_\parallel$ was thus not necessary, and equilibrium ordering could be compared directly among systems or under conditions in which $f_\parallel$ varied. Of course, the values of f_v produced in the present work are model-dependent quantities and reflect an interpretation based on the particular form of the probe orientational distribution function described above.

All parameter estimation was performed by application of a modified Gauss–Newton nonlinear least-squares algorithm (Johnson, 1983; Johnson & Frasier, 1985). Asymmetrical confidence intervals were estimated by this same software package in which the nonlinear variance space is searched so as to map out all parameter values which yield variances less than that which corresponds to a particular probability level. In the present work, 67% confidence limits were estimated because that level of confidence corresponds to approximately one standard deviation in the case of Gaussian distributions.

Results and Discussion

Fluorescence Lifetimes. Results of the total fluorescence intensity decay analysis indicate that both DPH and TMA–DPH intensity decays are substantially altered by the presence of unbleached rhodopsin in egg PC vesicles. When analyzed by the constrained two-population model, the presence of rhodopsin in these vesicles induces (1) a substantial increase in the derived fraction of short lifetime fluorophores, α_1, and (2) a reduction in the derived population lifetimes, τ_1 and τ_2 [see Appendix of the supplementary material (see paragraph at end of paper regarding supplementary material)]. This behavior is consistent with unbleached rhodopsin dynamically quenching probe fluorescence via probe-to-retinal energy transfer (Dencher & Heyn, 1983; Stubbs et al., 1976). In the variable acyl chain vesicles (egg PC, DOPC, and PAPC) containing differing amounts of cholesterol (0, ~15, and ~30 mol %), the presence of approximately 1 mol % unbleached rhodopsin consistently produces short-lifetime fractional amplitudes, α_1, greater than about 0.5 and derived population lifetimes considerably shorter than those observed in compositionally analogous rhodopsin-free vesicle systems [see Appendix and Straume and Litman (1987b) for comparison].

Characterization of DPH and TMA–DPH total fluorescence intensity decays by a discrete, two-population model better approximates fluorophore decay kinetics than does a single exponential model. Probe fluorescence in lipid bilayers, particularly in those in which energy-transfer acceptors, such as unbleached rhodopsin, are distributed, is very likely best represented by a continuous distribution of emitting species varying in their fluorescence lifetimes (Glaser et al., 1986). Characterization in terms of lifetime distributions, however, requires measurements at more than just a few modulation frequencies, as in the present work. The approximate nature implicit in discrete, biexponential fits of probe total fluorescence intensity decays therefore does not permit any direct physical interpretation of the derived population fractional amplitudes, α_i, and fluorescence lifetimes, τ_i. The rhodopsin-dependent increase in short-lifetime fluorophore content and decrease in derived population lifetimes do, however, suggest a redistribution of DPH and TMA–DPH fluorescence lifetimes toward shorter values.

Quantitation of the average fluorophore decay lifetime may be accomplished by considering the intensity-weighted mean fluorescence lifetime, $\tau(1)$. This parameter permits convenient interpretation of the effects of experimental variables (such as rhodopsin content, temperature, cholesterol content, and acyl chain composition, for example) on the average lifetime behavior of DPH and TMA–DPH. The approximately linear

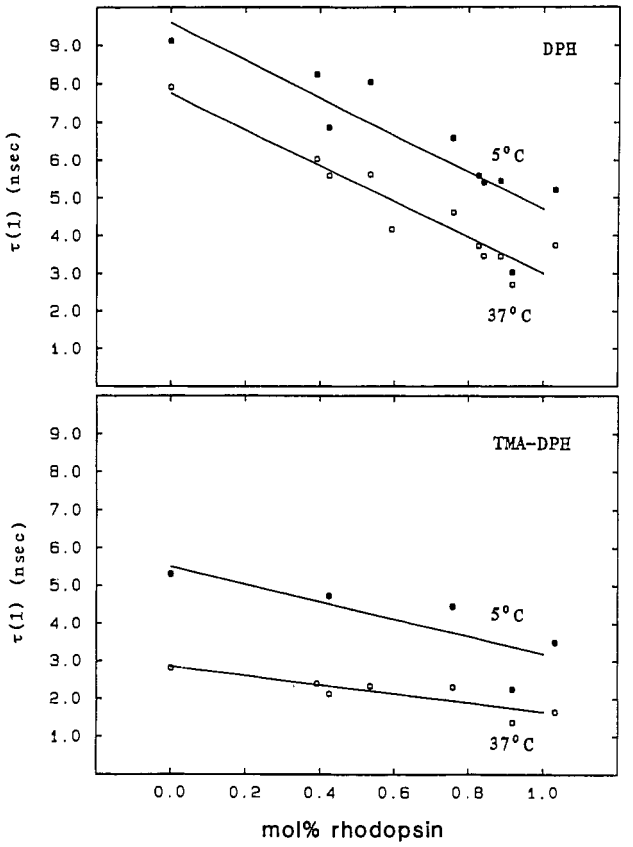

FIGURE 1: Intensity-weighted mean fluorescence lifetimes, $\tau(1)$, derived for DPH- (top) and TMA-DPH- (bottom) labeled egg PC-rhodopsin vesicles at 37 °C (open symbols) and 5 °C (closed symbols).

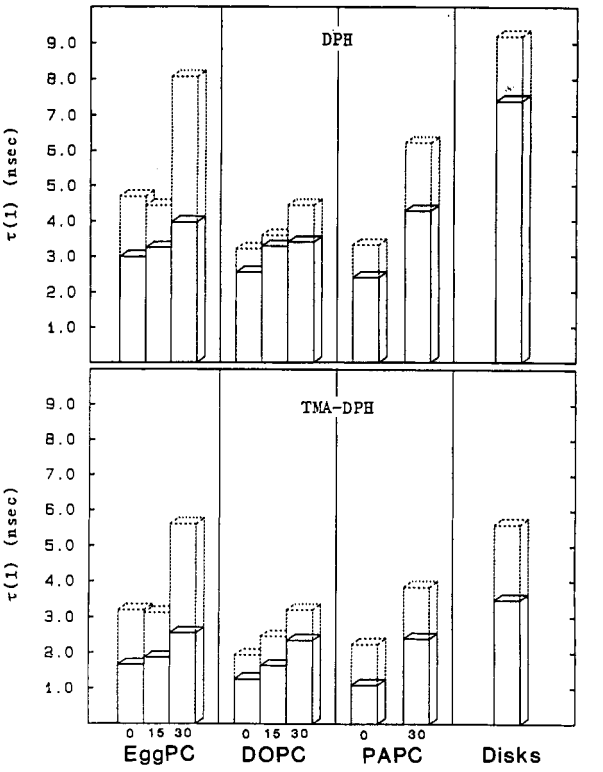

FIGURE 2: Intensity-weighted mean fluorescence lifetimes, $\tau(1)$, derived for DPH- (top) and TMA-DPH- (bottom) labeled vesicles at 37 °C (solid lines) and 5 °C (dotted lines) as a function of PC acyl chain composition and mole percent cholesterol.

decline of $\tau(1)$ for both DPH and TMA-DPH with increasing rhodopsin content in egg PC vesicles (see Figure 1) clearly indicates the presence of a dynamic quenching process which correlates directly with the protein content of these vesicles (Dencher & Heyn, 1983; Stubbs et al., 1976). The mean lifetimes of DPH and TMA-DPH observed in the variable acyl chain vesicle systems containing approximately 1 mol % rhodopsin and various amounts of cholesterol are considerably shorter than those observed in rhodopsin-free vesicles of the same lipid composition [see Figure 2 and Straume and Litman (1987b) for comparison]. Both probes exhibit increased values of $\tau(1)$ as the temperature is reduced, independent of rhodopsin content, cholesterol content, or acyl chain composition. Increasing the cholesterol content of rhodopsin-containing vesicles also induces longer mean fluorophore lifetimes for both DPH and TMA-DPH. TMA-DPH lifetimes show greater relative temperature-dependent and cholesterol-dependent sensitivity than do those of DPH. The same qualitative dependence of probe lifetimes on sample temperature and cholesterol content was observed in compositionally analogous rhodopsin-free vesicles (Straume & Litman, 1987a,b). In those experiments, increased probe lifetimes were interpreted as arising from reduced water penetrability into the lipid bilayers as a result of reduced lipid molecular flexibility under conditions of lower temperature or elevated cholesterol content. Reduced probe-water interactions make dynamic depopulation of fluorophore excited states by water less probable, resulting in longer probe lifetimes. Results from experiments utilizing other biophysical techniques support correlation of these temperature-dependent and cholesterol-dependent lifetime increases with reduced water penetrability into the bilayer as a result of a more ordered bilayer structure at lower temperatures and higher cholesterol levels, particularly at the headgroup and interfacial regions of the bilayer (the regions probed by TMA-DPH). The presence of rhodopsin in these liquid-crystalline PC vesicles does not appear to eliminate these temperature-dependent and cholesterol-dependent changes in lipid structure.

Another factor which may potentially contribute to these observed temperature-dependent and cholesterol-dependent lifetime changes in rhodopsin-containing bilayers must, however, be considered. Retinal in rhodopsin offers an absorption dipole roughly parallel to the plane of the bilayer (Chabre & Breton, 1979). As temperature is reduced or cholesterol content is increased, average lipid ordering is increased (see Equilibrium Ordering). This causes a net alignment of DPH and TMA-DPH emission dipoles with the bilayer normal. Such a redistribution of probe molecules will cause the energy-transfer donor and acceptor dipoles to deviate from parallel alignment leading to reduced energy-transfer efficiency. This produces less dynamic quenching of probe fluorescence and results in longer fluorophore lifetimes (Lakowicz, 1983). The greater relative sensitivity of mean probe lifetimes to changes in temperature or cholesterol content in these rhodopsin-containing vesicles than in compositionally analogous rhodopsin-free vesicles is consistent with changes in energy-transfer efficiency playing a role in this phenomenon.

The DOPC-rhodopsin vesicles display less temperature-dependent lifetime enhancement, independent of cholesterol content, than do the egg PC or PAPC vesicles. This suggests that, at low temperature, this diunsaturated PC-rhodopsin system permits greater penetration of water into the bilayer than do the mixed-chain egg PC or PAPC system. This would result in more frequent probe-water interactions thus promoting dynamic quenching of probe fluorescence and causing lifetimes to be shorter than would be the case in the absence of such interactions. Such acyl chain dependent differences were not apparent in compositionally analogous rhodopsin-free

vesicles (Straume & Litman, 1987a,b). This suggests that rhodopsin interacts less favorably with DOPC than with egg PC or PAPC. Other evidence exists supporting the preferential interaction of rhodopsin with saturated rather than unsaturated acyl chains (Zumbulyadis & O'Brien, 1979). The equilibrium order exhibited by the DOPC–rhodopsin vesicles is quite similar to that seen in the egg PC and PAPC systems, particularly in the presence of cholesterol, so it appears unlikely that a difference in energy-transfer efficiency could account for this acyl chain dependent difference in probe lifetimes.

The mean lifetime of DPH in disk membranes is somewhat longer than that observed in even the 30 mol % cholesterol containing vesicles. TMA–DPH lifetimes, however, do not show as much variation between disks and the 30 mol % cholesterol containing vesicles. This behavior is consistent with (1) a reduced frequency of quenching DPH–water interactions and (2) an unchanged frequency of TMA–DPH–water interactions in disks relative to that in the 30 mol % cholesterol containing PC vesicles. DPH resides within the hydrophobic bilayer interior (Shinitzky & Barenholz, 1978) while TMA–DPH is localized near the bilayer headgroup and interfacial regions (Engel & Prendergast, 1981; Prendergast et al., 1981). The mean lifetime results thus imply that the penetration of water into the hydrophobic region of the bilayer is limited to a greater extent in the disk membrane than it is in the 30 mol % cholesterol containing PC vesicles. The phospholipid headgroup composition of bovine ROS disk membranes includes 35–45 mol % PE and 10–15 mol % PS, primarily in the outer monolayer, and 35–45 mol % PC and 10–15 mol % cholesterol, primarily in the inner monolayer (Raubach et al., 1974; Sklar et al., 1979; Smith et al., 1977). The present work indicates no substantial differences in equilibrium or dynamic bilayer structure between disks and the PC vesicles. Differences in probe-to-retinal energy-transfer efficiency are therefore not likely the cause of the observed lifetime differences. The presence of charged PE and PS headgroups (at pH 7) may, however, be responsible for reducing the depth of water penetrability into disk membranes. More favorable water–headgroup interactions may occur in disks thus limiting the mobility of water molecules at the membrane surface. The presence of PE and PS headgroups may also restrict local lipid molecular fluctuations, such as acyl chain rotomers [see Straume and Litman (1987a,b)], which aid in transporting water into the disk membrane. This would limit the accessibility of water to regions nearer the bilayer surface relative to that which occurs in the PC vesicles. The considerable acyl chain heterogeneity that exists in disk membranes (Anderson & Maude, 1970; Anderson & Sperling, 1971; Borggreven et al., 1970; Miljanich et al., 1979; Nielsen et al., 1970; Poincelot & Abrahamson, 1970) may also contribute in some way to the observed lifetime differences, although the present experiments contribute no insight into such a possibility.

The same qualitative temperature dependence of $\tau(1)$ is observed for both DPH and TMA–DPH in disk membranes as in the reconstituted vesicles examined. Temperature reductions therefore further inhibit water penetrability into disk membranes, although the effect of increasing equilibrium order on the probe-to-retinal energy transfer efficiency must also be considered as a potential contributing factor to these temperature-dependent lifetime increases.

Equilibrium Ordering. At all temperatures examined, both the hydrophobic bilayer interior and the headgroup and interfacial regions of egg PC vesicles become more ordered as rhodopsin levels are increased. This is demonstrated by the reduction in the fractional volume derived for DPH and

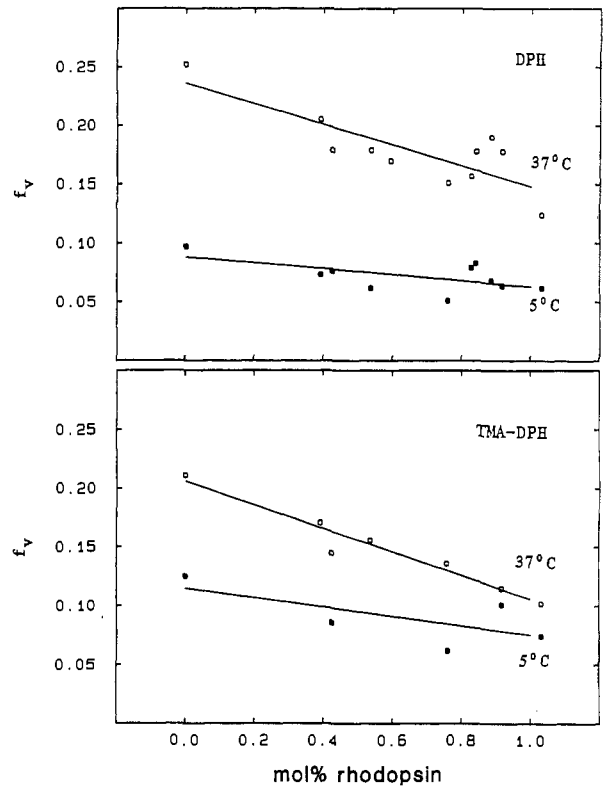

FIGURE 3: Fractional volumes, f_v, available for probe reorientational motion for DPH- (top) and TMA–DPH- (bottom) labeled egg PC–rhodopsin vesicles at 37 °C (open symbols) and 5 °C (closed symbols).

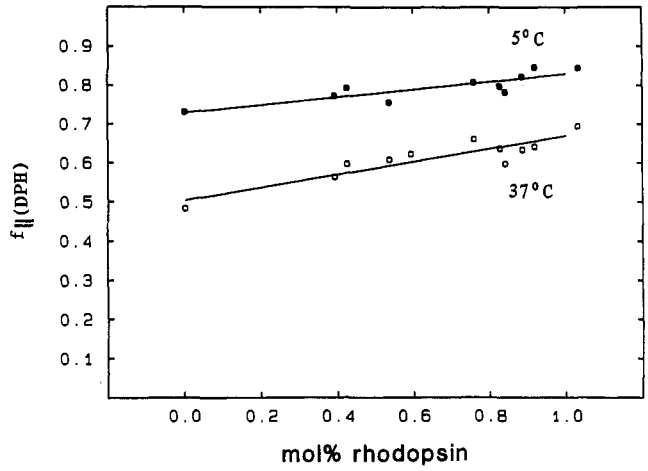

FIGURE 4: Fractions of DPH orientational distribution functions parallel to the bilayer normal, $f_{\parallel}$, i.e., parallel to the phospholipid acyl side chains, in egg PC–rhodopsin vesicles at 37 °C (open symbols) and 5 °C (closed symbols).

TMA–DPH reorientational motion as the vesicle rhodopsin content is increased (see Figure 3). Unimodal TMA–DPH orientational distributions are narrowed whereas bimodal DPH equilibrium orientations are primarily redistributed in favor of alignment with the bilayer normal while not experiencing much narrowing (see Figure 4 for DPH $f_{\parallel}$ values and the Appendix for probe θ_g values). The presence of approximately 1 mol % rhodopsin in the variable acyl chain vesicle systems also induces greater equilibrium lipid order (as quantified by the fractional volume parameter, f_v, in Figure 5) relative to compositionally analogous vesicles containing no rhodopsin [see Straume and Litman (1987b) for comparison]. This rhodopsin-dependent ordering is observed independent of acyl chain composition, cholesterol content, or temperature. Again, TMA–DPH orientational distributions are narrowed, and those

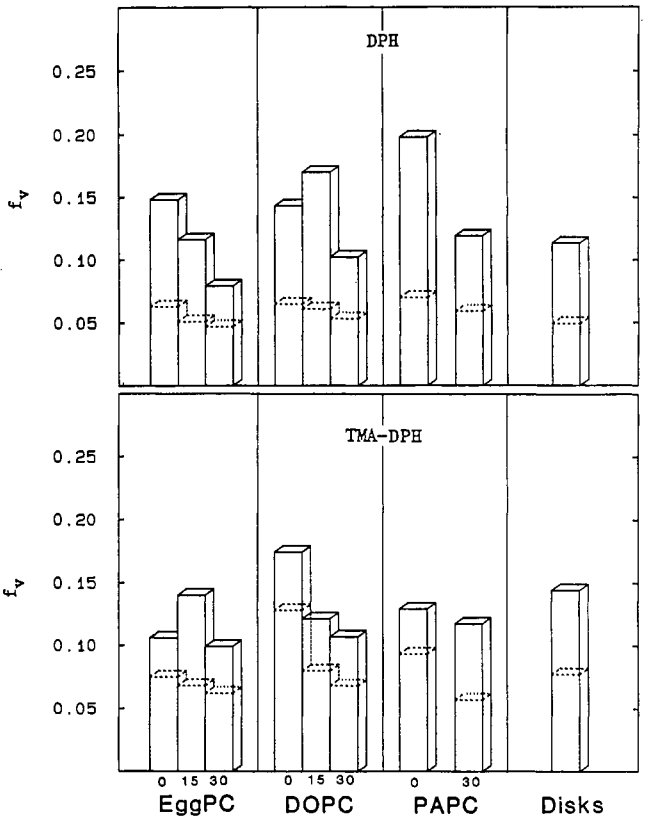

FIGURE 5: Fractional volumes, f_v, available for probe reorientational motion for DPH- (top) and TMA-DPH- (bottom) labeled vesicles at 37 °C (solid lines) and 5 °C (dotted lines) as a function of PC acyl chain composition and mole percent cholesterol.

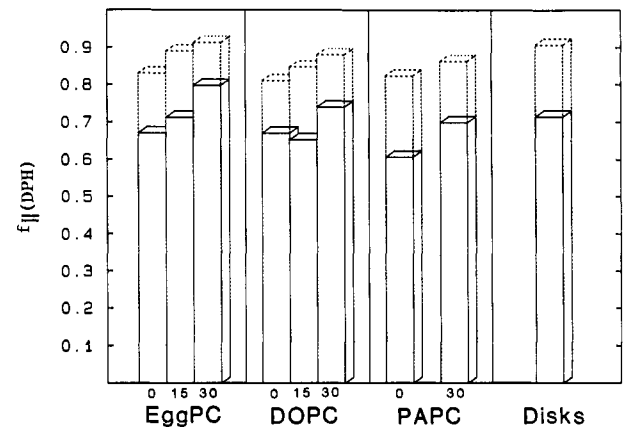

FIGURE 6: Fractions of DPH orientational distribution functions parallel to the bilayer normal, $f_{\parallel}$, i.e., parallel to the phospholipid acyl side chains, at 37 °C (solid lines) and 5 °C (dotted lines) as a function of PC acyl chain composition and mole percent cholesterol.

of DPH are narrowed to a small extent but primarily redistributed parallel to the bilayer normal [see Figure 6 for DPH $f_{\parallel}$ values, the Appendix for probe θ_g values, and Straume and Litman (1987b) for comparison with rhodopsin-free vesicles].

Lipid molecular motions are thus restricted at the headgroup and interfacial regions (as probed by TMA-DPH) indicative of increased lateral molecular packing density of the bilayer lipids in the presence of rhodopsin. The rhodopsin-induced redistribution of DPH orientational probability, on the other hand, suggests that free volume is reduced and equilibrium ordering is increased at the bilayer median. Rhodopsin spans the entire thickness of the bilayer (Hargrave et al., 1983; Ovchinnikov, 1982) and thus is expected to inhibit the extent of motional freedom available to phospholipid acyl chain termini resulting in a more extended average acyl chain configuration. The relative resistance of cholesterol-free DOPC–rhodopsin vesicles to experience rhodopsin-dependent ordering in the headgroup and interfacial regions again suggests that rhodopsin interacts less favorably with diunsaturated PC molecules, in the absence of cholesterol, than it does with mixed-chain lipids, consistent with the results of Zumbulyadis and O'Brien (1979). Upon inclusion of cholesterol to approximately 15 or 30 mol % levels, however, the equilibrium ordering detected in DOPC vesicles becomes similar to that found in the other systems examined.

Experiments using ESR and NMR techniques have shown that intrinsic membrane proteins exert an ordering influence on bilayer lipid molecular structure (Chapman, 1982; Deese et al., 1982; Fisher & Levy, 1981; Jost et al., 1973; Seelig & Seelig, 1980; Seelig et al., 1981; Utsumi et al., 1980). Analysis of experimental observations has led to interpretation in terms of lateral gradients of lipid structural order around some intrinsic membrane proteins but not around others. Different biophysical methods are capable of detecting lipid molecular order relative to different time scales. Comparisons among results obtained by various techniques suggest that exchange of bulk bilayer lipids with those adjacent to membrane proteins occurs on the order of 10^{-7}–10^{-5} s. Methods unable to discern molecular dynamics faster than approximately 10^{-5} s therefore do not detect multiple lipid populations differing in ordering properties. Methods capable of resolving lipid structural properties on a faster time scale, however, often infer the presence of a relatively immobilized lipid subpopulation around intrinsic membrane proteins.

The fluorescent probes DPH and TMA-DPH are expected to distribute throughout the lipid matrix of protein-containing vesicle systems thus experiencing all of the structural environments which may exist in the bilayer. Because these probes permit characterization of dynamic phenomena on the order of 10^{-9} s, their measured properties will not reflect averaging due to lateral exchange among lipid molecules in the bilayer. The present work, however, estimates only a single, homogeneous population of fluorophores with regard to their rotational depolarization properties. A rotational diffusion coefficient and either a unimodal equilibrium orientational distribution (for TMA-DPH) or a bimodal equilibrium orientational distribution (for DPH) fully define the dynamic and equilibrium depolarization properties of each of these probes. The present analysis thus simultaneously considers (1) the more ordered structural properties of any boundary lipid which may be present and (2) the structural properties of bulk lipid which is unaffected by the presence of protein in the membrane. Such an analysis will necessarily produce derived structural properties suggesting greater average lipid order. The observed rhodopsin-dependent increases in equilibrium lipid order therefore are consistent with, although not direct evidence for, the presence of lateral gradients of lipid order around rhodopsin molecules. Greater experimental determination of the systems considered in this work, by multifrequency measurements, for example (Lakowicz et al., 1985), would permit characterization of the measured system properties by a more complex and sophisticated analytical model. Such an approach would make possible interpretation of dynamic fluorescence depolarization phenomena in terms of multiple populations of rotating species (Davenport et al., 1986; Wang et al., 1986). Discrimination of gradients of lipid order around intrinsic membrane proteins might then be directly possible from fluorescence measurements as has been inferred from ESR and NMR studies.

Temperature reductions and increasing levels of cholesterol also induce more ordered equilibrium bilayer structure in

rhodopsin-containing vesicles as detected by both DPH and TMA–DPH. The temperature-dependent changes in equilibrium ordering observed in egg PC–rhodopsin vesicles occur across the entire range of rhodopsin levels examined. The ordering induced by reducing the temperature, however, is not as substantial in systems higher in protein content. This comes about because the protein-dependent lipid ordering is of greater magnitude at higher temperatures. When the effects of increasing cholesterol content on the structural properties of rhodopsin-containing vesicles are considered, it is seen that the bilayer interior of the variable acyl chain vesicle systems undergoes more substantial cholesterol-dependent ordering at higher temperatures than it does at lower temperatures, independent of acyl chain composition. The ordering of the bilayer interior induced by temperature reductions is therefore of greater magnitude at lower cholesterol levels, as well. Rhodopsin and cholesterol thus each inhibit lipid molecular freedom more substantially under conditions in which the lipid matrix is inherently more highly disordered, i.e., at higher temperatures. This suggests that a limiting degree of order in the liquid-crystalline state can be attained by either increasing protein content, increasing cholesterol content, or decreasing temperature.

The ordering experienced by DPH molecules in response to temperature reductions or increasing levels of cholesterol arises from a substantial redistribution of DPH molecules in favor of alignment with the bilayer normal accompanied by a small reduction in the width of the probe orientational probability distribution. Increasing the cholesterol content and lowering the sample temperature thus each promotes ordering of the bilayer interior, just as increasing levels of rhodopsin do. Cholesterol and lower temperatures therefore also induce more extended average acyl chain structure at the bilayer median thereby reducing the free volume available for molecular motion. Increasing cholesterol levels and temperature reductions contribute to increases in the lateral lipid molecular packing density of the bilayer surface region, as well. Many of the responses observed in these rhodopsin-containing vesicles are qualitatively similar to those observed in compositionally analogous protein-free systems (Straume & Litman, 1987a,b), so the presence of rhodopsin in these vesicles does not eliminate these temperature-dependent and cholesterol-dependent changes in lipid structural properties.

Native disk membranes labeled with DPH exhibit equilibrium ordering of the hydrophobic bilayer interior most similar to that observed in PC recombinants containing approximately 30 mol % cholesterol. Both the derived Gaussian distribution widths, θ_g, and the fraction of DPH parallel, $f_\parallel$, agree closely thus yielding very similar fractional volumes, f_v. The interfacial and headgroup regions of disks, as probed by TMA–DPH, however, display somewhat less equilibrium lipid order than do the 30 mol % cholesterol containing recombinants. These observations suggest that the lipid heterogeneity present in disk membranes accounts for some additional equilibrium lipid structural disorder at the bilayer surface relative to that of recombinant vesicles composed only of PC, cholesterol, and rhodopsin.

Two additional differences between disks and these reconstituted vesicles should be pointed out: (1) disks contain approximately 1.5 mol % rhodopsin versus approximately 1 mol % in the recombinants, and (2) disks contain rhodopsin oriented in a unique direction relative to the inner and outer monolayers of the membrane whereas the recombinants very likely contain rhodopsin molecules oriented with their C-termini oriented toward the inner and outer monolayers in roughly equal proportions. The higher rhodopsin content in disks would be expected to further increase equilibrium lipid order relative to that occurring in a compositionally analogous membrane containing only 1 mol % rhodopsin. This implies that the headgroup and/or acyl chain heterogeneity in disks may contribute to maintaining some additional equilibrium lipid disorder relative to that present in the reconstituted PC vesicles examined. Uniform versus random vectorial distributions of rhodopsin in the membrane bilayer do not immediately suggest any effect on bilayer structure, although such a possibility cannot be ruled out by the present experimental observations.

The equilibrium and dynamic probe orientational properties derived from the present analysis implicitly take into account probe fluorescence intensity decay behavior. Fluorescence lifetime parameters are derived prior to analysis of anisotropy decay parameters and are included as input parameters into the depolarization analysis. Therefore, any changes in fluorescence lifetimes brought about by changes in vesicle composition or temperature are fully accounted for during derivation of probe equilibrium and dynamic reorientational properties. For example, a reduction in DPH lifetime would have the effect of increasing the steady-state anisotropy of DPH if everything else in some hypothetical system remained constant. However, a dynamic analysis, such as that performed in the present studies, would extract from all of the experimental observations on this same hypothetical system (i.e., probe fluorescence lifetime parameters, steady-state anisotropy, and dynamic depolarization parameters) the correct and unaltered equilibrium and dynamic probe reorientational properties.

Experiments to test this were performed on native bovine ROS disk membranes which were (1) unbleached, (2) bleached, (3) bleached in the presence of hydroxylamine (to shift the retinal absorption peak considerably blue by forming retinal oxime), and (4) bleached in the presence of hydroxylamine and then extracted with fatty acid free bovine serum albumin (to remove as much of the retinal oxime as possible). The absorption spectra of samples 1–4 were substantially different both in extinction and in wavelength of maximum absorbance. The extent of overlap between the absorption spectra of these samples and the emission spectra of DPH and TMA–DPH therefore also was quite different for each of these four samples. The lifetime properties of the probes thus varied considerably and systematically on going from sample 1 to sample 4. Fractional amplitudes of the short-lifetime component decreased and population lifetimes increased on going from sample 1 to sample 4 and encompassed approximately the same range of values encountered in the studies reported here. However, the dynamic reorientational analysis produced effectively identical parameter values characteristic of the equilibrium order and the dynamics of probe rotational diffusion for each of these four samples. Differences in energy-transfer efficiency, or any other phenomena causing lifetime differences, for that matter, therefore will not invalidate the results obtained from this depolarization analysis.

Rotational Dynamics. Rates of DPH and TMA–DPH depolarizing motion in egg PC vesicles fail to show any discernible correlation with mole percent rhodopsin at any of the temperatures examined (see Appendix). Lipid molecular dynamics therefore appear not to be affected by the protein either in the hydrophobic bilayer core or at the headgroup and interfacial regions of egg PC vesicles. No differences in rotational dynamics are apparent between the bilayer core and the bilayer surface region in any of the vesicle systems exam-

ined. Rotational depolarization kinetics do, however, appear to be slightly accelerated by increasing cholesterol levels in the variable acyl chain vesicle systems, although not to nearly the same extent as in compositionally analogous vesicles containing no rhodopsin (Straume & Litman, 1987b). The presence of approximately 1 mol % rhodopsin therefore largely suppresses the substantial cholesterol-dependent acceleration of probe rotational dynamics observed in protein-free vesicles. Precise characterization of rates of probe depolarizing motion is difficult with limited-frequency measurements giving rise to some scatter among the values derived in different experiments. While little or no dependence of depolarization kinetics is seen on rhodopsin content, acyl chain composition, cholesterol content, or depth within the bilayer, all of the samples considered in this work display slower depolarization kinetics for both DPH and TMA–DPH as sample temperatures are reduced. Values of $D_\perp$ for DPH range from 0.18–0.39 ns^{-1} at 37 °C to 0.07–0.28 ns^{-1} at 5 °C. $D_\perp$ for TMA–DPH ranges from 0.17–0.53 ns^{-1} at 37 °C to 0.06–0.22 ns^{-1} at 5 °C.

Native disk membranes exhibit lipid dynamics very similar to those observed in the reconstituted vesicles. Again, lipid dynamics as detected by DPH and TMA–DPH are approximately the same, suggesting no dependence of lipid dynamics on depth within the bilayer. Lower temperatures promote slower probe depolarization in disks as was the case in the reconstituted PC–cholesterol–rhodopsin vesicles. Attempts to more thoroughly interpret relatively subtle differences among the derived $D_\perp$ values would not be justified due to the inherent difficulty in precisely quantifying this parameter.

Conclusions

We present here conclusions from the series of studies in which the compositional complexity of reconstituted vesicles was systematically increased (Straume & Litman, 1987a,b), culminating with the present report. DPH and TMA–DPH fluorescence lifetimes were analyzed by a constrained, discrete biexponential model (Straume & Litman, 1987a). Probe depolarization properties were analyzed by a recently developed, higher order model which (1) derives orthogonal, bimodal orientational distributions for DPH, (2) derives unimodal orientational distributions for TMA–DPH, and (3) characterizes depolarization kinetics by a single rotational diffusion coefficient (Straume & Litman, 1987a).

Probe lifetimes are generally increased by (1) lesser degrees of acyl chain unsaturation, (2) increasing levels of cholesterol, and (3) reductions in temperature. In the absence of rhodopsin, long-lifetime fluorophores account for the majority of the fluorescence intensity decay amplitude. When rhodopsin is present, probe-to-retinal energy transfer increases the relative contribution of short-lifetime fluorophores to a majority and causes lifetimes to be reduced. The relative proportions of short- and long-lifetime fluorophores are not affected by changes in acyl chain unsaturation, cholesterol content, or temperature. Conditions which promote longer lifetimes are interpreted as altering membrane structural properties in ways so as to permit less penetration of water into the bilayer. Lifetime results suggest that diunsaturated DOPC molecules interact less favorably with rhodopsin than do mixed-chain PCs. Also, native disk membranes appear to reduce the penetration of water into the hydrocarbon region of the bilayer to a greater extent than do any of the recombinant vesicles examined, perhaps as a result of the relatively large proportion of PE and PS phospholipids in disk membranes.

The equilibrium order of both the hydrophobic bilayer core and of the headgroup and interfacial regions of the bilayer is increased by (1) lesser degrees of acyl chain unsaturation, (2) increasing levels of cholesterol, (3) increasing levels of rhodopsin, and (4) reductions in temperature. Increases in order are characterized by narrower probe orientational distributions and, in the case of DPH, by redistribution of probe molecules in favor of alignment with the bilayer normal. The lateral molecular packing density in the plane of the bilayer is therefore increased as equilibrium order increases. Redistribution of DPH parallel to the bilayer normal indicates that the acyl chain terminal region at the bilayer median adopts a more extended average acyl chain configuration as equilibrium order increases. The order of the bilayer interior is more sensitive to changes in vesicle composition and temperature than are the bilayer headgroup and interfacial regions. The equilibrium order results again suggest that diunsaturated DOPC molecules interact less favorably with rhodopsin than do mixed-chain PCs, but this difference is eliminated upon including 15 or 30 mol % cholesterol. Native disk membranes exhibit nearly the same equilibrium order as that observed in cholesterol-containing PC–rhodopsin recombinant vesicles.

Probe rotational dynamics appear to be independent of acyl chain composition and rhodopsin content, but in the absence of rhodopsin, cholesterol promotes considerable acceleration of probe reorientational dynamics. The presence of 1 mol % rhodopsin, however, largely eliminates this cholesterol-dependent acceleration of probe depolarizing motion. DPH and TMA–DPH exhibit approximately the same rotational diffusion coefficients, suggesting that there is no dependence of lipid dynamics on depth within the bilayer. Reductions in temperature consistently slow probe depolarizing motions. Disk membranes display the same rates of probe motion as do the recombinant rhodopsin-containing PC vesicles.

Knowledge of the effects of acyl chain composition, cholesterol content, rhodopsin content, and temperature on the equilibrium and dynamic structure of unsaturated acyl chain vesicles aids in developing a more thorough understanding of composition–structure relationships which exist in biological membranes. Although native bovine ROS disk membranes display considerably more compositional heterogeneity than any of the recombinant vesicle systems examined in these studies, the nature of some of the molecular interactions occurring in natural membranes has been addressed. The preparation of reconstituted vesicles containing up to approximately 30 mol % cholesterol corresponds to the limit necessary to mimic the bilayer environment of rhodopsin in disk membranes if the approximately 10–15 mol % cholesterol found in disks is completely asymmetrically distributed into one monolayer of the disk membrane. Studies currently in progress to determine the equilibrium and dynamic structural and functional properties of rhodopsin in reconstituted model vesicle systems of defined composition will permit correlation of the functional response of this membrane protein to the physical properties of its bilayer environment (Morton et al., 1986). Such systematic studies on compositionally defined reconstituted model vesicles will therefore help advance the current understanding of the involvement of variables such as acyl chain composition, cholesterol content, and headgroup composition on biomembrane physical properties as well as their specific influences on regulation of membrane-associated protein structure and function.

Acknowledgments

We thank Dr. M. L. Johnson for providing general-purpose software and assistance in nonlinear least-squares analysis and graphic output. We also thank J. Murphy and Dr. M. L. Jackson for technical assistance and expertise in the preparation of the samples.

Supplementary Material Available

Appendix containing tabulations of derived fluorescence intensity decay and dynamic depolarization parameters for DPH and TMA-DPH as a function of temperature, rhodopsin content, acyl chain composition, and cholesterol content for large, unilamellar, octyl glucoside dilution recombinant vesicles and native bovine rod outer segment disk membranes (14 pages). Ordering information is given on any current masthead page.

Registry No. DOPC, 10015-85-7; PAPC, 74936-60-0; H_2O, 7732-18-5; cholesterol, 57-88-5.

References

Akino, T., & Tsuda, M. (1979) *Biochim. Biophys. Acta 556*, 61–71.

Ameloot, M., Hendrickx, H., Herreman, W., Pottel, H., van Cauwelaert, F., & van der Meer, W. (1984) *Biophys. J. 46*, 525–539.

Anderson, R. E., & Maude, M. B. (1970) *Biochemistry 9*, 3624–3628.

Anderson, R. E., & Sperling, L. (1971) *Arch. Biochem. Biophys. 144*, 673–677.

Applebury, M. L. (1984) *Vision Res. 24*, 1445–1454.

Applebury, M. L., Zuckerman, D. M., Lamola, A. A., & Jovin, T. M. (1974) *Biochemistry 13*, 3448–3458.

Baker, N., & Wilson, L. (1966) *J. Lipid Res. 7*, 341–348.

Baldwin, P. A., & Hubbell, W. L. (1985a) *Biochemistry 24*, 2624–2632.

Baldwin, P. A., & Hubbell, W. L. (1985b) *Biochemistry 24*, 2633–2639.

Barrow, D. A., & Lentz, B. R. (1985) *Biophys. J. 48*, 221–234.

Bartlett, G. R. (1959) *J. Biol. Chem. 234*, 466–468.

Benga, G., & Holmes, R. P. (1984) *Prog. Biophys. Mol. Biol. 43*, 195–257.

Borggreven, J. M. P. M., Daemen, F. J. M., & Bonting, S. L. (1970) *Biochim. Biophys. Acta 202*, 374–381.

Brown, M. F., & Williams, G. D. (1985) *J. Biochem. Biophys. Methods 11*, 71–81.

Chabre, M., & Breton, J. (1979) *Vision Res. 19*, 1005–1018.

Chapman, D. (1982) *Biol. Membr. 4*, 327–366.

Chen, L. A., Dale, R. E., Roth, S., & Brand, L. (1977) *J. Biol. Chem. 252*, 2163–2169.

Davenport, L., Knutson, J. R., & Brand, L. (1986) *Biochemistry 25*, 1811–1816.

Deese, A. J., Dratz, E. A., Dahlquist, F. W., & Paddy, M. R. (1981) *Biochemistry 20*, 6420–6247.

Deese, A. J., Dratz, E. A., Hymel, L., & Fleischer, S. (1982) *Biophys. J. 37*, 207–216.

Dencher, N. A., & Heyn, M. P. (1983) *Biophys. J. 43*, 39–45.

Devaux, P. F., & Seigneuret, M. (1985) *Biochim. Biophys. Acta 822*, 63–125.

Engel, L. W., & Prendergast, F. G. (1981) *Biochemistry 20*, 7338–7345.

Estep, T. N., Mountcastle, D. B., Biltonen, R. L., & Thompson, T. E. (1978) *Biochemistry 17*, 1984–1989.

Fisher, T. H., & Levy, G. C. (1981) *Chem. Phys. Lipids 28*, 7–23.

Fukuda, M. N., Papermaster, D. S., & Hargrave, P. A. (1979) *J. Biol. Chem. 254*, 8201–8207.

Glaser, M., Fiorini, R., Wang, S., Valentino, M., & Gratton, E. (1986) *Biophys. J. 49*, 307a.

Hargrave, P. A., McDowell, J. H., Curtis, D. R., Wang, J. K., Juszczak, E., Fong, S.-L., Mohana Rao, J. K., & Argos, P. (1983) *Biophys. Struct. Mech. 9*, 235–244.

Henselman, R. A., & Cusanovich, M. A. (1974) *Biochemistry 13*, 5199–5203.

Hildenbrand, K., & Nicolau, C. (1979) *Biochim. Biophys. Acta 553*, 365–377.

Jackson, M. L., & Litman, B. J. (1985) *Biochim. Biophys. Acta 812*, 369–376.

Jackson, M. L., Schmidt, C. F., Lichtenberg, D., Litman, B. J., & Albert, A. D. (1982) *Biochemistry 21*, 4576–4582.

Jahnig, F., Vogel, H., & Best, L. (1982) *Biochemistry 21*, 6790–6798.

Johnson, M. L. (1983) *Biophys. J. 44*, 101–106.

Johnson, M. L., & Frasier, S. G. (1985) *Methods Enzymol. 117*, 301–342.

Jost, P. C., Griffith, O. H., Capaldi, R. A., & Vanderkooi, G. (1973) *Proc. Natl. Acad. Sci. U.S.A. 70*, 480–484.

Kawato, S., Kinosita, K., Jr., & Ikegami, A. (1977) *Biochemistry 16*, 2319–2324.

Kinosita, K., Jr., Kataoka, R., Kimura, Y., Gotoh, O., & Ikegami, A. (1981a) *Biochemistry 20*, 4270–4277.

Kinosita, K., Jr., Kawato, S., Ikegami, A., Yoshida, S., & Orii, Y. (1981b) *Biochim. Biophys. Acta 647*, 7–17.

Klausner, R. D., Kleinfeld, A. M., Hoover, R. L., & Karnovsky, M. J. (1980) *J. Biol. Chem. 255*, 1286–1295.

Lakowicz, J. R. (1980) *J. Biochem. Biophys. Methods 2*, 91–119.

Lakowicz, J. R. (1981) in *Spectroscopy in Biochemistry* (Bell, J. E., Ed.) pp 195–245, CRC, Boca Raton, FL.

Lakowicz, J. R. (1983) *Principles of Fluorescence Spectroscopy*, Plenum, New York.

Lakowicz, J. R., & Prendergast, F. G. (1978) *Science (Washington, D.C.) 200*, 1399–1401.

Lakowicz, J. R., Prendergast, F. G., & Hogan, D. (1979) *Biochemistry 18*, 508–519.

Lakowicz, J. R., Cherek, H., Maliwal, B. P., & Gratton, E. (1985) *Biochemistry 24*, 376–383.

Lipari, G., & Szabo, A. (1980) *Biophys. J. 30*, 489–506.

Litman, B. J. (1982) *Methods Enzymol. 81*, 150–166.

Litman, B. J., Kalisky, O., & Ottolenghi, M. (1981) *Biochemistry 20*, 631–634.

Lowry, O. H., Rosebrough, N. J., Farr, A. L., & Randall, R. J. (1951) *J. Biol. Chem. 193*, 265.

Miljanich, G. P., Sklar, L. A., White, D. L., & Dratz, E. A. (1979) *Biochim. Biophys. Acta 552*, 294–306.

Moore, N. F., Patzer, E. J., Barenholz, Y., & Wagner, R. R. (1977) *Biochemistry 16*, 4708–4715.

Morton, R. W., Straume, M., Miller, J. L., & Litman, B. J. (1986) *Biophys. J. 49*, 277a.

Nielsen, N. C., Fleischer, S., & McConnell, D. G. (1970) *Biochim. Biophys. Acta 211*, 10–19.

O'Brien, D. F., Costa, L. F., & Ott, R. A. (1977) *Biochemistry 16*, 1295–1303.

Ovchinnikov, Y. A. (1982) *FEBS Lett. 148*, 179–191.

Parasassi, T., Conti, F., Glaser, M., & Gratton, E. (1984) *J. Biol. Chem. 259*, 14011–14017.

Pink, D. A., Chapman, D., Laidlaw, D. J., & Weidmer, T. (1984) *Biochemistry 23*, 4051–4058.

Poincelot, R. P., & Abrahamson, E. W. (1970) *Biochemistry 9*, 1820–1825.

Prendergast, F. G., Haugland, R. P., & Callahan, P. J. (1981) *Biochemistry 20*, 7333–7338.

Raubach, R. A., Nemes, P. P., & Dratz, E. A. (1974) *Exp. Eye Res. 18*, 1–11.

Salesse, R., & Garnier, J. (1984) *Mol. Cell. Biochem. 60*, 17–31.

Seelig, J., & Seelig, A. (1980) *Q. Rev. Biophys. 13*, 19–61.
Seelig, J., Tamm, L., Hymel, L., & Fleischer, S. (1981) *Biochemistry 20*, 3922–3932.
Shinitzky, M., & Barenholz, Y. (1978) *Biochim. Biophys. Acta 515*, 367–394.
Sklar, L. A., Miljanich, G. P., Bursten, S. L., & Dratz, E. A. (1979) *J. Biol. Chem. 254*, 9583–9591.
Slater, T. F. (1984) *Methods Enzymol. 105*, 283–293.
Smith, H. G., Stubbs, G. W., & Litman, B. J. (1975) *Exp. Eye Res. 20*, 211–217.
Smith, H. G., Fager, R. S., & Litman, B. J. (1977) *Biochemistry 16*, 1399–1405.
Straume, M., & Litman, B. J. (1987a) *Biochemistry 26*, 5113–5120.
Straume, M., & Litman, B. J. (1987b) *Biochemistry 26*, 5121–5126.
Stubbs, C. D. (1983) *Essays Biochem. 19*, 1–39.
Stubbs, C. D., Kouyama, T., Kinosita, K., Jr., & Ikegami, A. (1981) *Biochemistry 20*, 4257–4262.
Stubbs, C. D., Kinosita, K., Jr., Munkonge, F., Quinn, P. J., & Ikegami, A. (1984) *Biochim. Biophys. Acta 775*, 374–380.
Stubbs, G. W., & Litman, B. J. (1978) *Biochemistry 17*, 220–225.
Stubbs, G. W., Litman, B. J., & Barenholz, Y. (1976) *Biochemistry 15*, 2766–2772.
Sunamoto, J., Baba, Y., Iwamoto, K., & Kondo, H. (1985) *Biochim. Biophys. Acta 833*, 144–150.
Szabo, A. (1984) *J. Chem. Phys. 81*, 150–167.
Thompson, T. E., & Huang, C. (1986) in *Physiology of Membrane Disorder*, 2nd ed. (Andrioli, T. E., Hoffman, J. F., Fanestil, D. D., & Schultz, S. G., Eds.) pp 25–44, Plenum, New York.
Utsumi, H., Tunggal, B. D., & Stoffel, W. (1980) *Biochemistry 19*, 2385–2390.
van Blitterswijk, W. J., van Hoevan, R. P., & van der Meer, B. W. (1981) *Biochim. Biophys. Acta 644*, 323–332.
van der Meer, W., Pottel, H., Herreman, W., Ameloot, M., Hendrickx, H., & Schroder, H. (1984) *Biophys. J. 46*, 515–523.
van de Ven, M., van Ginkel, G., & Levine, Y. K. (1984) *Biochem. Biophys. Res. Commun. 123*, 352–357.
Vogel, H., & Jahnig, F. (1985) *Proc. Natl. Acad. Sci. U.S.A. 82*, 2029–2033.
Vos, M. H., Kooyman, R. P. H., & Levine, Y. K. (1983) *Biochem. Biophys. Res. Commun. 116*, 462–468.
Wang, S., Glaser, M., & Gratton, E. (1986) *Biophys. J. 49*, 307a.
Wong, P. T. T. (1984) *Annu. Rev. Biophys. Bioeng. 13*, 1–24.
Yeagle, P. L. (1984) *Prog. Clin. Biol. Res. 159*, 153–175.
Zannoni, C., Arcioni, A., & Cavatorta, P. (1983) *Chem. Phys. Lipids 32*, 179–250.
Zumbulyadis, N., & O'Brien, D. F. (1979) *Biochemistry 18*, 5427–5432.

Rotational Dynamics of Actin†

William H. Sawyer,* Amanda G. Woodhouse, Joseph J. Czarnecki,‡ and Edward Blatt§
Russell Grimwade School of Biochemistry, University of Melbourne, Parkville, Victoria 3052, Australia
Received November 13, 1987; Revised Manuscript Received June 9, 1988

ABSTRACT: The rotational diffusion of actin was studied with the technique of time-resolved phosphorescence anisotropy using actin labeled at Cys-374 with erythrosin iodoacetamide. Immediately after the polymerization of actin was initiated, the correlation time increased sharply, passing through a maximum at 5 min and then declined to low values. F-Actin at equilibrium showed no anisotropy decay. The results were interpreted as indicating the initial formation of short mobile filaments which became increasingly immobile as elongation proceeded, leaving a decay which was dominated by shorter filaments. Some of these short filaments could have arisen by fragmentation of longer filaments. Eventually, the shorter filaments themselves became immobilized by entanglement within the gel matrix. The infinite-time anisotropy increased during polymerization, reflecting a smaller range of angular motion of the probe brought about by restricted torsional motion on the submicrosecond time scale. The results were compared with the length distribution of actin filaments revealed by electron microscopy [Kawamura, M., & Maruyama, K. (1970) *J. Biochem.* (*Tokyo*) *67*, 437–457]. Polymerization in the presence of 1 μM cytochalasin B abolished the maximum in the correlation time profile and tended to prevent the immobilization of filaments by favoring shorter capped filaments which retained considerable rotational freedom. Addition of spectrin dimer to F-actin caused an increase in the time-invariant anisotropy. Subsequent additions of spectrin-binding proteins (erythrocyte bands 2.1 and 4.1) caused further increases in the anisotropy in a concentration-dependent manner, suggesting additional restriction of submicrosecond torsional motions. The results suggest that actin filaments within nonmuscle cells are rotationally immobile particularly if they are cross-linked by actin-binding proteins.

Microtubules, intermediate filaments, and microfilaments play an important role in determining cell shape and motility and the disposition and movement of subcellular organelles. Together with their associated proteins, they make up a cytoskeletal scaffolding on which is arrayed a number of cytoplasmic enzymes. Although the term "cytoskeleton" implies a relatively rigid arrangement of structural units of limited flexibility, it is more likely that cytoskeletal elements possess degrees of internal and global motion that permit deformation of cell shape without rupture of the cell membrane and

† This work was supported by the Australian Research Grants Scheme.
‡ Present address: ICI Diagnostics, 5 Guest St., Hawthorn, Victoria 3122, Australia.
§ Present address: CSIRO Division of Applied Organic Chemistry, GPO Box 4331, Melbourne, Victoria 3001, Australia.

0006-2960/88/0427-7733$01.50/0